Specifics of impurity effects in ferropnictide superconductors

Y. G. Pogorelov,[1,*] M. C. Santos,[2] and V. M. Loktev[3]
[1]*IFIMUP-IN, Departamento de Física, Universidade do Porto, Porto, Portugal*
[2]*Departamento de Física, Universidade de Coimbra, R. Larga, P-3004-535 Coimbra, Portugal*
[3]*Bogolyubov Institute for Theoretical Physics, NAN of Ukraine, 14b Metrologichna str., 03143 Kiev, Ukraine*
(Received 26 May 2011; revised manuscript received 7 September 2011; published 7 October 2011)

Effects of impurities and disorder on quasiparticle spectrum in superconducting iron pnictides are considered. The possibility of occurrence of localized energy levels due to impurities within the superconducting gap and the related modification of band structure, including the emergence of narrow bands of extended quasiparticle states near impurity levels, is analyzed. The evolution of a superconducting state with an impurity concentration is traced and some specific effects of the modified quasiparticle spectrum on the superconducting order parameter and other observable characteristics are discussed.

DOI: 10.1103/PhysRevB.84.144510 PACS number(s): 74.70.Xa, 74.62.Dh, 74.62.En

I. INTRODUCTION

The recent discovery of superconductivity (SC) with a rather high critical temperature in the family of doped ferropnictide compounds[1,2] has motivated a great interest in these materials (see reviews in Refs. 3 and 4). Unlike the extensively studied cuprate family,[5] which presents insulating properties in their initial undoped state, the undoped LaOFeAs compound is a semimetal. As established in previous physical and chemical studies (see, e.g., Refs. 6 and 7), this material has a layered structure, where the SC state is supported by the FeAs layer with a two-dimensional (2D) square lattice of Fe atoms and with As atoms located out of plane, above or below the centers of square cells (Fig. 1). Its electronic structure, relevant for constructing microscopic SC models, have been explored with high-resolution angle-resolved photoemission spectroscopy (ARPES) techniques.[8,9] Their results indicate the multiple connected structure of the Fermi surface, consisting of electron and hole pockets and an absence of nodes in both electron and hole spectrum gaps,[8] suggesting that these systems display the so-called extended s-wave (also called $s_{\pm}$wave) SC order, changing the order parameter sign between electron and hole segments.[13]

To study band structure, first-principles numeric calculations are commonly used, outlining the importance of Fe atomic d orbitals. The calculations show that SC in these materials is associated with Fe atoms in the layer plane, represented in Fig. 1 by their orbitals and the related hopping amplitudes. The dominance of Fe atomic $3d$ orbitals in the density of states (DOS) of the LaOFeAs compound near its Fermi surface was demonstrated by local density approximation (LDA) calculations.[10–15] It was then concluded that multiorbital effects are important for the electronic excitation spectrum in the SC state, causing the formation of two spectrum gaps: by electron and hole pockets at the Fermi surface. To explain the observed SC properties, it is suggested that these materials may reveal an unconventional pairing mechanism, beyond the common electron-phonon scheme.[16–19] In general, a total of five atomic orbitals for each iron in the LaOFeAs compound can be involved, however, ways to reduce this basis are sought, in order to simplify analytical and computational work. Some authors[20,21] have suggested that it is sufficient to consider only d_{xz} and d_{yz} orbitals. Building such a minimal coupling model based on two orbitals, one is able to adjust the model parameters (energy hopping and chemical potential) to obtain a Fermi surface with the same topology as in the first-principles calculations of band structure. Even though it fails to reproduce some finer features of the electronic spectrum,[22,23] this minimal coupling scheme is favored, because of its technical simplicity, to be chosen as the basis for study of impurity effects in LaOFeAs which would hardly be tractable in more involved frameworks.

Having established the SC-state parameters, an important class of problems can be considered about the effects of disorder, in particular, by impurities, on the system electronic properties, and this issue has also been studied for doped ferropnictides. Like the situation in doped perovskite cuprates, here impurity centers can either result from the dopants, necessary to form the very SC state, or from foreign atoms and other local defects in the crystalline structure. Within the minimal coupling model, the interesting possibility of localized impurity levels appearing within SC gaps in doped LaOFeAs was indicated, even for the simplest, so-called isotopic (or nonmagnetic) type of impurity perturbation.[24,25] This finding marks an essential difference from traditional SC systems with an s-wave gap on a single-connected Fermi surface, where such perturbations are known not to produce localized impurity states and thus to have no sizable effect on SC order, according to the Anderson theorem.[26] In the presence of localized quasiparticle states by isolated impurity centers, the next important issue is the possibility of collective behavior of such states at high enough impurity concentrations. This possibility was studied long ago for electronic quasiparticles in doped semiconducting systems[27] and also for other types of quasiparticles in pnononic, magnonic, excitonic, etc., spectra under impurities,[28] establishing conditions for collective (including coherent) behavior of impurity excitations, with striking effects in the observable properties of such systems. As for high-T_c -doped cuprates, it is known that their d-wave symmetry of SC order permits only impurity resonances in the spectrum of quasiparticles,[29,30] not their true localization, and hinders notable collective effects on their observable properties. To our knowledge, no consistent study on collective impurity effects is known for doped ferropnictide systems at present, and this defines the main emphasis of the present work.

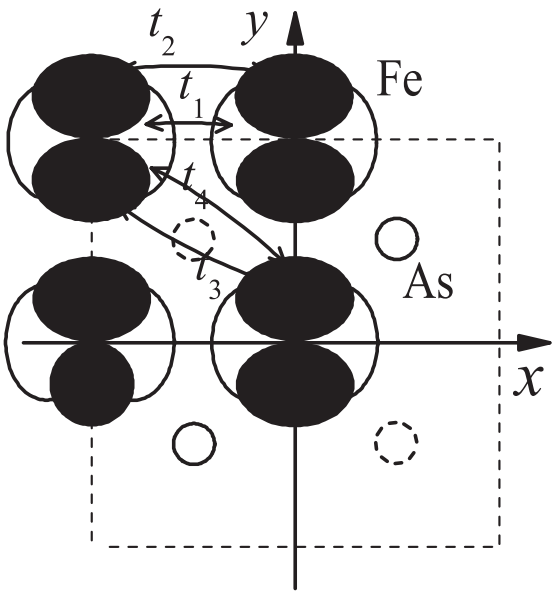

FIG. 1. Schematics of a FeAs layer in the LaoFeAs compound with d_{xz} (white) and d_{yz} (dark) Fe orbitals and the Fe-Fe hopping parameters in the minimal coupling model. Note that the hoppings between next-nearest neighbors ($t_{3,4}$) are mediated by As orbitals (out of the Fe plane).

Namely, we develop an analysis of these systems, using Green function (GF) techniques, similar to those for doped cuprate SC systems,[31] the minimal coupling model with two orbitals for ferropnictide electronic structure, and the simplest isotopic type for impurity perturbation. The structure of the quasiparticle spectrum near in-gap impurity levels at finite impurity concentrations, conditions for emergence of specific branches of collective excitations in this region of the spectrum, and expected observable effects of such spectrum restructuring are discussed.

II. MODEL HAMILTONIAN AND GREEN FUNCTIONS

For the minimal coupling model in Fig. 1, the hopping Hamiltonian H_t is written in the local orbital basis as

$$\begin{aligned} H_t = -\sum_{\mathbf{n},\sigma}[&t_1(x^\dagger_{\mathbf{n},\sigma}x_{\mathbf{n}+\delta_x,\sigma} + y^\dagger_{\mathbf{n},\sigma}y_{\mathbf{n}+\delta_y,\sigma} + \text{h.c.}) \\ &+ t_2(x^\dagger_{\mathbf{n},\sigma}x_{\mathbf{n}+\delta_y,\sigma} + y^\dagger_{\mathbf{n},\sigma}y_{\mathbf{n}+\delta_x,\sigma} + \text{h.c.}) \\ &+ t_3(x^\dagger_{\mathbf{n},\sigma}x_{\mathbf{n}+\delta_x+\delta_y,\sigma} + x^\dagger_{\mathbf{n},\sigma}x_{\mathbf{n}+\delta_x-\delta_y,\sigma} \\ &+ y^\dagger_{\mathbf{n},\sigma}y_{\mathbf{n}+\delta_x+\delta_y,\sigma} + y^\dagger_{\mathbf{n},\sigma}y_{\mathbf{n}+\delta_x-\delta_y,\sigma} + \text{h.c.}) \\ &+ t_4(x^\dagger_{\mathbf{n},\sigma}y_{\mathbf{n}+\delta_x+\delta_y,\sigma} + y^\dagger_{\mathbf{n},\sigma}x_{\mathbf{n}+\delta_x+\delta_y,\sigma} \\ &- x^\dagger_{\mathbf{n},\sigma}y_{\mathbf{n}+\delta_x-\delta_y,\sigma} - y^\dagger_{\mathbf{n},\sigma}x_{\mathbf{n}+\delta_x-\delta_y,\sigma} + \text{h.c.})]. \end{aligned} \quad (1)$$

where $x_{\mathbf{n},\sigma}$ and $y_{\mathbf{n},\sigma}$ are the Fermi operators for d_{xz} and d_{yz} Fe orbitals with spin σ on the $\mathbf{n}$ lattice site and the vectors $\boldsymbol{\delta}_{x,y}$ point to its nearest neighbors in the square lattice. Passing to the operators of orbital plane waves $x_{\mathbf{k},\sigma} = N^{-1/2}\sum_{\mathbf{n}} e^{i\mathbf{k}\cdot\mathbf{n}}x_{\mathbf{n},\sigma}$ (with a number N of lattice cells) and analogous $y_{\mathbf{k},\sigma}$, and defining an "orbital" 2-spinor $\psi^\dagger(\mathbf{k},\sigma) = (x_{\mathbf{k},\sigma}, y_{\mathbf{k},\sigma})$, one can expand the spinor Hamiltonian in quasimomentum:

$$H_t = \sum_{\mathbf{k},\sigma}\psi^\dagger(\mathbf{k},\sigma)\hat{h}_t(\mathbf{k})\psi(k,\sigma). \quad (2)$$

Here the 2×2 matrix,

$$\hat{h}_t(\mathbf{k}) = \varepsilon_{+,\mathbf{k}}\hat{\sigma}_0 + \varepsilon_{-,\mathbf{k}}\hat{\sigma}_3 + \varepsilon_{xy,\mathbf{k}}\hat{\sigma}_1, \quad (3)$$

includes the Pauli matrices $\hat{\sigma}_i$ and the energy functions

$$\varepsilon_{\pm,\mathbf{k}} = \frac{\varepsilon_{x,\mathbf{k}} \pm \varepsilon_{y,\mathbf{k}}}{2}, \quad (4)$$

with

$$\begin{aligned} \varepsilon_{x,\mathbf{k}} &= -2t_1\cos k_x - 2t_2\cos k_y - 4t_3\cos k_x\cos k_y, \\ \varepsilon_{y,\mathbf{k}} &= -2t_1\cos k_y - 2t_2\cos k_x - 4t_3\cos k_x\cos k_y, \\ \varepsilon_{xy,\mathbf{k}} &= -4t_4\sin k_x\sin k_y. \end{aligned}$$

The optimum fit for the calculated band structure within the minimum coupling model is attained with the set of hopping parameters (in $|t_1|$ units), $t_1 = -1.0$, $t_2 = 1.3$, $t_3 = t_4 = -0.85$, and with the choice of Fermi energy (chemical potential at zero temperature) $\varepsilon_F = 1.45$.[15] The $\hat{h}_t$ matrix is diagonalized by the standard unitary transformation:

$$\hat{U}(\mathbf{k}) = \begin{pmatrix} \cos\theta_\mathbf{k}/2 & -\sin\theta_\mathbf{k}/2 \\ \sin\theta_\mathbf{k}/2 & \cos\theta_\mathbf{k}/2 \end{pmatrix},$$

with $\theta_\mathbf{k} = \arctan(\varepsilon_{xy,\mathbf{k}}/\varepsilon_{-,\mathbf{k}})$, transforming it from an orbital to a sub-band basis:

$$\hat{h}_b(\mathbf{k}) = \hat{U}^\dagger(\mathbf{k})\hat{h}_t(\mathbf{k})\hat{U}(\mathbf{k}) = \begin{pmatrix} \varepsilon_{e,\mathbf{k}} & 0 \\ 0 & \varepsilon_{h,\mathbf{k}} \end{pmatrix}. \quad (5)$$

The energy eigenvalues in Eq. (4),

$$\varepsilon_{h,e}(\mathbf{k}) = \varepsilon_{+,\mathbf{k}} \pm \sqrt{\varepsilon^2_{xy,\mathbf{k}} + \varepsilon^2_{-,\mathbf{k}}}, \quad (6)$$

correspond to the two sub-bands in the normal-state spectrum that define electron and hole pockets of the Fermi surface, respectively. There are two segments of each type, defined by the equations $\varepsilon_{e,h}(\mathbf{k}) = \mu$, as shown in Fig. 2. We note that both functions $\cos\theta_\mathbf{k}$ and $\sin\theta_\mathbf{k}$ change their sign around these segments, corresponding to their "azimuthal dependencies" around characteristic points in the Brillouin zone (Fig. 2), so that integrals of these functions with some azimuthal-independent factors over the relevant vicinity of the Fermi surface practically vanish and are neglected beside such integrals of fully azimuthal-independent functions in the analysis below.

The adequate basis for constructing the SC state is generated by the operators of electron and hole sub-bands:

$$\begin{aligned} \alpha_{\mathbf{k},\sigma} &= x_{\mathbf{k},\sigma}\cos\theta_\mathbf{k}/2 - y_{\mathbf{k},\sigma}\sin\theta_\mathbf{k}/2, \\ \beta_{\mathbf{k},\sigma} &= y_{\mathbf{k},\sigma}\cos\theta_\mathbf{k}/2 + x_{\mathbf{k},\sigma}\sin\theta_\mathbf{k}/2, \end{aligned} \quad (7)$$

giving rise to the "multiband-Nambu" 4-spinors $\Psi^\dagger_\mathbf{k} = (\alpha^\dagger_{\mathbf{k},\uparrow}, \alpha_{-\mathbf{k},\downarrow}, \beta^\dagger_{\mathbf{k},\uparrow}, \beta_{-\mathbf{k},\downarrow})$ and to a 4×4 extension of the Hamiltonian, Eq. (2), in the form

$$H_s = \sum_{\mathbf{k},\sigma}\Psi^\dagger_\mathbf{k}\hat{h}_s(\mathbf{k})\Psi_\mathbf{k}, \quad (8)$$

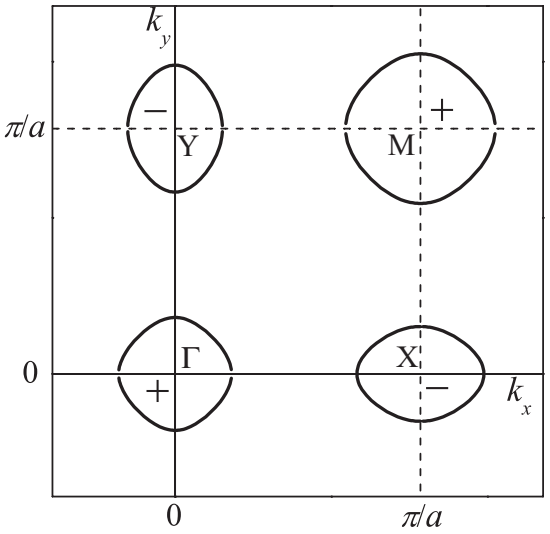

FIG. 2. Electron (−) and hole (+) segments of the Fermi surface in the normal state of the model system with the electronic spectrum from Eq. (5). The center of the first Brillouin zone is displaced by $(\pi/2a,\pi/2a)$ to fully include all the segments around four characteristic points Γ, X, M, and Y in this zone.

where the 4×4 matrix

$$\hat{h}_s(\mathbf{k}) = \hat{h}_b(\mathbf{k}) \otimes \hat{\tau}_3 + \Delta_{\mathbf{k}} \hat{\sigma}_0 \otimes \hat{\tau}_1$$

includes the Pauli matrices $\hat{\tau}_i$ acting on the Nambu (particle-antiparticle) indices in Ψ-spinors and $\hat{h}_b(\mathbf{k})$ is defined by Eq. (5). The simplified form for the extended s-wave SC order is realized with the definition of the gap function by constant values, $\Delta_{\mathbf{k}} = \Delta$ on electron segments and $\Delta_{\mathbf{k}} = -\Delta$ on hole segments.

The electronic dynamics of this system is determined by the (Fourier-transformed) GF 4×4 matrices[28,31,32]

$$\hat{G}_{\mathbf{k},\mathbf{k}'} = \langle\langle \Psi_{\mathbf{k}} | \Psi^{\dagger}_{\mathbf{k}} \rangle\rangle = i \int_{-\infty}^{0} dt e^{i\varepsilon t/\hbar} \langle\{\Psi_{\mathbf{k}}(t), \Psi^{\dagger}_{\mathbf{k}'}(0)\}\rangle, \quad (9)$$

whose energy argument ε is understood as $\varepsilon - i0$ and $\langle\{A(t), B(0)\}\rangle$ is the quantum statistical average with Hamiltonian H of the anticommutator of Heisenberg operators. From the equation of motion,

$$\varepsilon \hat{G}_{\mathbf{k},\mathbf{k}'} = \hbar \delta_{\mathbf{k},\mathbf{k}'} \hat{\sigma}_0 \otimes \tau_0 + \langle\langle [\Psi_{\mathbf{k}}, H] | \Psi^{\dagger}_{\mathbf{k}'} \rangle\rangle, \quad (10)$$

the explicit GF for the unperturbed SC system with the Hamiltonian H_s, Eq. (7), is diagonal in quasimomentum, $\hat{G}_{\mathbf{k},\mathbf{k}'} = \delta_{\mathbf{k},\mathbf{k}'} \hat{G}^0_{\mathbf{k}}$ and

$$\hat{G}^0_{\mathbf{k}} = \frac{\varepsilon \hat{\tau}_0 + \varepsilon_e(\mathbf{k}) \hat{\tau}_3 + \Delta \hat{\tau}_1}{2D_{e,\mathbf{k}}} \otimes \hat{\sigma}_+ + \frac{\varepsilon \hat{\tau}_0 + \varepsilon_h(\mathbf{k}) \hat{\tau}_3 - \Delta \hat{\tau}_1}{2D_{h,\mathbf{k}}} \otimes \hat{\sigma}_-, \quad (11)$$

where $\hat{\sigma}_{\pm} = (\hat{\sigma}_0 \pm \hat{\sigma}_3)/2$ and the secular denominators $D_{i,\mathbf{k}} = \varepsilon^2 - \varepsilon_i^2(\mathbf{k}) - \Delta^2$ for $i = e,h$. In what follows, we use the energy reference to the Fermi level ε_{F} and approximate the segments of the Fermi surface by some circles of radius k_i around the characteristic points $\mathbf{K}_i$ in the Brillouin zone, so that the dispersion laws $\varepsilon_j(\mathbf{k}) = \varepsilon_{\mathrm{F}} + \xi_{j,\mathbf{k}}$ permit linearization of the quasiparticle dispersion close to the Fermi level as $\xi_{j,\mathbf{k}} \approx \hbar v_j \left(|\mathbf{k} - \mathbf{K}_j| - k_i\right)$. Generally, the Fermi wave numbers k_j and related Fermi velocities v_j for $j = e$ and h can differ somewhat for a given choice of hopping parameters and chemical potential, but for simplicity, we neglect this difference and consider their single values $k_j = k_{\mathrm{F}}$ and $v_j = v_{\mathrm{F}}$.

III. IMPURITY PERTURBATION AND SELF-ENERGY

We pass to the impurity problem, where the above Hamiltonian is addedby the local perturbation terms due to nonmagnetic impurities[24] on random sites $\mathbf{p}$ in the Fe square lattice with an on-site energy shift V:

$$H_{\mathrm{imp}} = V \sum_{\mathbf{p},\sigma} (x^{\dagger}_{\mathbf{p},\sigma} x_{\mathbf{p},\sigma} + y^{\dagger}_{\mathbf{p},\sigma} y_{\mathbf{p},\sigma}). \quad (12)$$

Without loss of generality, the parameter V can be taken as positive, and for GF calculations, this perturbation is suitably expressed in the multiband-Nambu basis,

$$H_{\mathrm{imp}} = \frac{1}{N} \sum_{\mathbf{p},\mathbf{k},\mathbf{k}'} e^{i(\mathbf{k}'-\mathbf{k})\cdot\mathbf{p}} \Psi^{\dagger}_{\mathbf{k}} \hat{V}_{\mathbf{k},\mathbf{k}'} \Psi_{\mathbf{k}'}, \quad (13)$$

through the 4×4 scattering matrix $\hat{V}_{\mathbf{k},\mathbf{k}'} = V \hat{U}^{\dagger}_{\mathbf{k}} \hat{U}_{\mathbf{k}'} \otimes \tau_3$. As follows from the above expression for $\hat{U}_{\mathbf{k}}$, this matrix involves either "intraband" or "interband" elements.[33] The latter type of scattering could lead to a possible transformation from the $s_{\pm}$ to a competing s_{++} SC order (with the same sign of order parameter on both Fermi pockets) under the impurity effect.[34] However, as shown below, such a possibility is effectively eliminated for the chosen local perturbation type, due to the specific quasimomentum $\mathbf{k}$ dependence of the scattering elements, unlike their constancy, postulated in Ref. 34.

Within the approach in Refs. 28 and 31, the solution for Eq. (9) with the perturbed Hamiltonian $H_s + H_i$ can be obtained in different forms, suitable for different types of states, band-like (extended) or localized. All these forms result from the basic equation of motion,

$$\hat{G}_{\mathbf{k},\mathbf{k}'} = \delta_{\mathbf{k},\mathbf{k}'} \hat{G}^0_{\mathbf{k}} + \frac{1}{N} \sum_{\mathbf{p},\mathbf{k}''} e^{i(\mathbf{k}''-\mathbf{k})\cdot\mathbf{p}} \hat{G}^0_{\mathbf{k}} \hat{V}_{\mathbf{k},\mathbf{k}''} \hat{G}_{\mathbf{k}'',\mathbf{k}'}, \quad (14)$$

by specific routines of iterating this equation for the "scattered" GFs $\hat{G}_{\mathbf{k}'',\mathbf{k}'}$.

Thus, the algorithm, where the next iteration step *never* applies to the scattered GFs already present after previous steps, e.g., that with $\mathbf{k}'' = \mathbf{k}$ in Eq. (14), leads to the so-called fully renormalized form, suitable for band-like states,

$$\hat{G}_{\mathbf{k}} = \left[\left(\hat{G}^0_{\mathbf{k}} \right)^{-1} - \hat{\Sigma}_{\mathbf{k}} \right]^{-1}, \quad (15)$$

where the self-energy matrix $\hat{\Sigma}_{\mathbf{k}}$ is expressed by the related group expansion (GE):

$$\hat{\Sigma}_{\mathbf{k}} = c\hat{T}_{\mathbf{k}}(1 + c\hat{B}_{\mathbf{k}} + \dots). \quad (16)$$

Here $c = \sum_{\mathbf{p}} N^{-1}$ is the impurity concentration (per Fe site) and the T matrix results from all the multiple scatterings by a single impurity:

$$\hat{T}_{\mathbf{k}} = \hat{V}_{\mathbf{k},\mathbf{k}} + \frac{1}{N}\sum_{\mathbf{k}'\neq\mathbf{k}} \hat{V}_{\mathbf{k},\mathbf{k}'}\hat{G}^0_{\mathbf{k}'}\hat{V}_{\mathbf{k}',\mathbf{k}} + \frac{1}{N^2}\sum_{\mathbf{k}'\neq\mathbf{k},\mathbf{k}''\neq\mathbf{k},\mathbf{k}'} \hat{V}_{\mathbf{k},\mathbf{k}'}\hat{G}^0_{\mathbf{k}'}\hat{V}_{\mathbf{k}',\mathbf{k}''}\hat{G}^0_{\mathbf{k}''}\hat{V}_{\mathbf{k}'',\mathbf{k}} + \dots . \quad (17)$$

The term next to the unity in parentheses in Eq. (16),

$$\hat{B}_{\mathbf{k}} = \sum_{\mathbf{n}} (\hat{A}_{\mathbf{n}} e^{-i\mathbf{k}\cdot\mathbf{n}} + \hat{A}_{\mathbf{n}}\hat{A}_{-\mathbf{n}})(1 - \hat{A}_{\mathbf{n}}\hat{A}_{-\mathbf{n}})^{-1}, \quad (18)$$

describes the effects of indirect interactions in pairs of impurities, separated by vector $\mathbf{n}$, in terms of interaction matrices $\hat{A}_{\mathbf{n}} = \hat{T}_{\mathbf{k}}\sum_{\mathbf{k}'\neq\mathbf{k}} e^{i\mathbf{k}'\cdot\mathbf{n}}\hat{G}_{\mathbf{k}'}$. Besides this restriction on summation, multiple sums in the products like $\hat{A}_{\mathbf{n}}\hat{A}_{-\mathbf{n}}$ never contain coincident quasimomenta. Equation (18) presents the first nontrivial GE term and the rest of its terms omitted in Eq. (14) correspond to the contributions from groups of three or more impurities.[28]

An alternative iteration routine for Eq. (14) applies it to *all* the scattered GFs; this results in the so-called nonrenormalized form, suitable for localized states:

$$\hat{G}_{\mathbf{k}} = \hat{G}^0_{\mathbf{k}} + \hat{G}^0_{\mathbf{k}}\hat{\Sigma}^0_{\mathbf{k}}\hat{G}^0_{\mathbf{k}}. \quad (19)$$

Here the nonrenormalized self-energy GE, $\hat{\Sigma}^0_{\mathbf{k}} = c\hat{T}(1 + c\hat{B}^0_{\mathbf{k}} + \cdots)$, differs from the above renormalized one in the absence of restrictions in quasimomentum sums for interaction matrices $\hat{A}^0_{\mathbf{n}} = \hat{T}_{\mathbf{k}}\sum_{\mathbf{k}'} e^{i\mathbf{k}'\cdot\mathbf{n}}\hat{G}^0_{\mathbf{k}'}$ and their products.

In the first step, we restrict GE to the common T-matrix level, providing the conditions for localized quasiparticle states with in-gap energy levels to appear at single impurities,[21] and study certain (narrow) energy bands of specific collective states that can be formed near these levels at finite impurity concentrations. In the next step, the criteria for such collective states really to exist in a disordered SC system follow from the analysis of nontrivial GE terms. We note that the presence of renormalized GFs $\hat{G}_{\mathbf{k}'}$ in the above interaction matrices is just necessary for adequate treatment of interaction effects over the in-gap bands.

IV. *T* MATRIX AND QUASIPARTICLE STATES

The T matrix, Eq. (16), is readily simplified taking into account that $\hat{V}_{\mathbf{k},\mathbf{k}} = V\hat{\sigma}_0 \otimes \hat{\tau}_3$ and introducing the integrated GF matrix:

$$\hat{G}_0 = \frac{1}{N}\sum_{\mathbf{k}} \hat{U}_{\mathbf{k}}\hat{G}^0_{\mathbf{k}}U^{\dagger}_{\mathbf{k}} = \varepsilon[g_e(\varepsilon)\hat{\sigma}_+ + g_h(\varepsilon)\hat{\sigma}_-] \otimes \hat{\tau}_0.$$

This diagonal form (that is, restricted only to the "intraband" matrix elements) follows directly from the aforementioned cancellation of the integrals with $\cos\theta_{\mathbf{k}}$ and $\sin\theta_{\mathbf{k}}$ that appear in the interband matrix elements of $\hat{U}_{\mathbf{k}}\hat{G}^0_{\mathbf{k}}U^{\dagger}_{\mathbf{k}}$. Therefore, we do not consider below that SC order can change its type under impurity effects.

Respectively, the functions $g_j(\varepsilon) = N^{-1}\sum_{\mathbf{k}} D^{-1}_{j,\mathbf{k}}$ for $j = e,h$ are approximated near the Fermi level, $|\varepsilon - \varepsilon_{\mathrm{F}}| \lesssim \Delta$, as

$$g_j(\varepsilon) \approx -\frac{\pi\rho_j}{\sqrt{\Delta^2 - \varepsilon^2}}. \quad (20)$$

Here $\rho_j = m_j a^2/(2\pi\hbar^2)$ are the Fermi densities of states for respective sub-bands (in parabolic approximation for their dispersion laws), and by assumed identity of all segments of the Fermi surface, they can also be considered identical, $\rho_j = \rho_{\mathrm{F}}$. Omitted terms in Eq. (16) are of higher orders in the small parameter $|\varepsilon|/\varepsilon_{\mathrm{F}} \ll 1$.

Then the momentum-independent T matrix is explicitly written as

$$\hat{T} = \gamma^2\frac{\varepsilon - \varepsilon_0\hat{\tau}_3}{\varepsilon^2 - \varepsilon_0^2}, \quad (21)$$

where $\varepsilon_0 = \Delta/\sqrt{1+v^2}$ defines the in-gap impurity level[21] through the dimensionless impurity perturbation parameter $v = \pi\rho_{\mathrm{F}}V$, and $\gamma^2 = v^2V\varepsilon_0^2/\Delta$ is the effective constant of coupling between localized and band quasiparticles. Evidently, Eq. (21) is only valid in a narrow enough vicinity of ε_0.

At finite c, using this T matrix in Eq. (14), we obtain, from the condition $\det\hat{G}^{-1}_{\mathbf{k}} = 0$[32], the formal dispersion equation expressed through dispersion of normal quasiparticles $\xi_{\mathbf{k}} = \varepsilon_{\mathbf{k}} - \varepsilon_{\mathrm{F}}$ (but neglecting the energy level width due to the effects of indirect interaction between impurities by higher GE terms):

$$D_{\mathbf{k}}(\varepsilon) = \varepsilon^2 - \xi^2_{\mathbf{k}} - \Delta^2 - \frac{2c\gamma^2(\varepsilon^2 - \varepsilon_0\xi_{\mathbf{k}})}{\varepsilon^2 - \varepsilon_0^2} = 0. \quad (22)$$

Its solutions, shown in Fig. 3 as a function of the quasimomentum argument $\xi = \xi_{\mathbf{k}}$, display a peculiar multiband structure. First, it includes four modified bands $\pm\varepsilon_b(\pm\xi)$, slightly shifted with respect to the unperturbed SC quasiparticle bands $\pm\sqrt{\Delta^2 + \xi^2}$, according to the basic function:

$$\varepsilon_b(\xi) \approx \sqrt{\Delta^2 + \xi^2} + c\gamma^2\frac{\Delta^2 + \xi^2 - \varepsilon_0\xi}{\sqrt{\Delta^2 + \xi^2}\left(\xi^2 + \xi_0^2\right)}, \quad (23)$$

with $\xi_0^2 = \Delta^2 - \varepsilon_0^2$. It should be noted that these sub-bands for opposite signs of their argument ξ in fact refer to excitations around different segments (by electron and holes) of the Fermi surface, but for clarity they are presented in Fig. 3 in the same ξ reference. Besides these ε_b bands, four (narrow) in-gap bands $\pm\varepsilon_i(\pm\xi)$ also appear, generated close to $\pm\varepsilon_0$ by finite concentrations of impurities, according to

$$\varepsilon_i(\xi) \approx \varepsilon_0 + c\gamma^2\frac{\xi - \varepsilon_0}{\xi^2 + \xi_0^2}. \quad (24)$$

As follows from Eq. (21), the $\varepsilon_j(\xi)$ band is located between its extrema $\varepsilon_{\max} = \varepsilon_0 + c\gamma^2\varepsilon_0/(\Delta + \varepsilon_0)$ at $\xi_+ = \varepsilon_0 + \Delta$ and $\varepsilon_{\min} = \varepsilon_0 - c\gamma^2\varepsilon_0/(\Delta - \varepsilon_0)$ at $-\xi_- = \varepsilon_0 - \Delta$. The energy and momentum shifts of the extremal points by Eqs. (20) and (21) and Fig. 3 are specific for the impurity effect on the multiband initial spectrum and they contrast with a simpler situation for an impurity level near the edge of a single-quasiparticle band.[28]

All these spectrum bands would contribute to the overall DOS by related quasiparticles: $\rho(\varepsilon) = (4\pi N)^{-1}\mathrm{Im}\,\mathrm{Tr}\sum_{\mathbf{k}}\hat{G}_{\mathbf{k}}$. The more common contributions here come from the ε_b

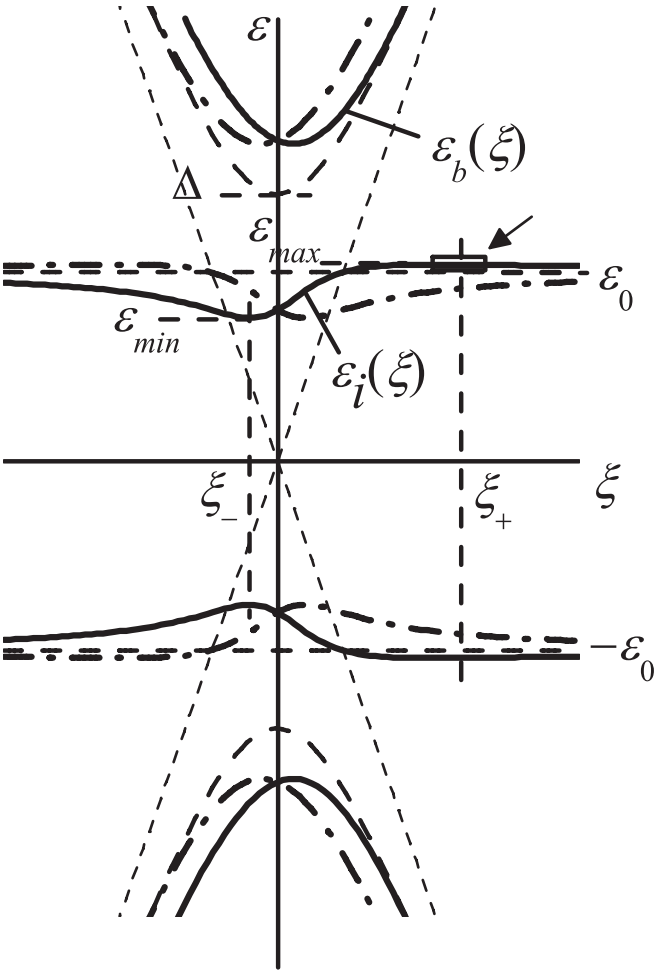

FIG. 3. Dispersion laws for band-like quasiparticles in the T-matrix approximation, neglecting their finite lifetime, at a specific choice of impurity parameters $v = 1$, $c = 0.1\Delta^2/\gamma^2$. The argument ξ composes all specific $\xi_j = \hbar v_F(|\mathbf{k} - \mathbf{K}_j| - k_F)$ for quasimomentum $\mathbf{k}$ near each jth characteristic point in the Brillouin zone [see the text after Eq. (23)], so that solid lines present the bands near electron-like segments of the Fermi surface, and dash-dotted lines those near hole-like segments. Nonperturbed SC quasiparticle bands and single-impurity localized levels are shown by dashed lines. The narrow rectangle around the top of the ε_i band (shown by the arrow) delimits the region in Fig. 5.

bands and they can be expressed through the Bardeen-Cooper-Schrieffer (BCS) DOS in pure crystal,[35] $\rho_{BCS}(\varepsilon,\Delta) = \rho_F\varepsilon/\sqrt{\varepsilon^2 - \Delta^2}$, as follows:

$$\rho_b(\varepsilon) \approx \left(1 - \frac{c\gamma^2}{\varepsilon^2 - \varepsilon_0^2}\right)\rho_{BCS}(\varepsilon,\Delta_c), \tag{25}$$

at $\varepsilon^2 \geqslant \Delta_c^2 = \Delta^2 + 2c\gamma^2\varepsilon_0^2/(\Delta^2 - \varepsilon_0^2)$. The first factor on the left-hand side of Eq. (25) describes a certain reduction in the BCS DOS, especially when the energy argument is close to the gap limits, and the shift of its gap argument is due to the quantum-mechanical repulsion between the band and the impurity levels.

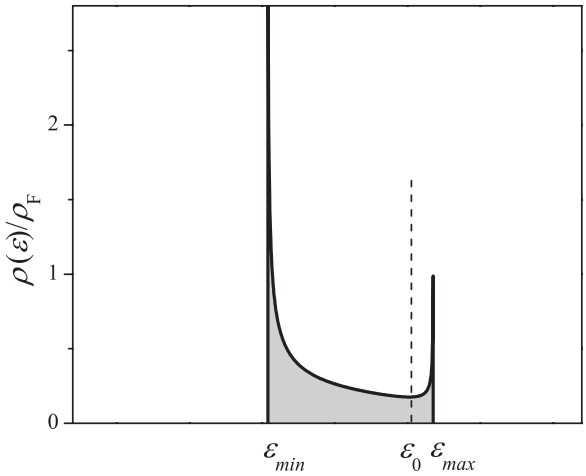

FIG. 4. Density of states in the narrow in-gap band near the impurity level ε_0 (dashed line) for the case in Fig. 3.

More peculiar is the contribution to DOS from the ε_i bands, written as

$$\rho_i(\varepsilon) \approx \frac{\rho_F}{v}\frac{\varepsilon^2 - \varepsilon_0^2 - c\gamma^2}{\sqrt{\left(\varepsilon_{max}^2 - \varepsilon^2\right)\left(\varepsilon^2 - \varepsilon_{min}^2\right)}}, \tag{26}$$

at $\varepsilon_{min}^2 \leqslant \varepsilon^2 \leqslant \varepsilon_{max}^2$, and presented in Fig. 4.

The effects of both ε_b band shifts and ε_i band formation can have important repercussions for the physical behavior of a disordered SC system and they are considered below. But before this, we need to analyze the criteria for the quasiparticles considered actually to exist, especially close to the limits of corresponding bands.

V. GROUP EXPANSION AND COHERENCE CRITERIA

Let us now study the crossover from band to localized states near the limits of ε_i bands, say, for definiteness, its upper limit ε_{max}. Supposing the actual energy $\varepsilon < \varepsilon_{max}$ to be within the range of band states, we use the fully renormalized self-energy matrix, Eq. (16), up to the GE pair term, $c^2\hat{T}\hat{B}_{\mathbf{k}}$, which will add a certain finite imaginary part $\Gamma_i(\xi)$ to the dispersion law $\varepsilon = \varepsilon_i(\xi)$, Eq. (23). Then the known Ioffe-Regel-Mott criterion[36,37] for the state at this energy to be really band-like (also called extended) is written as

$$\varepsilon_{max} - \varepsilon \gg \Gamma_i(\varepsilon). \tag{27}$$

To simplify calculation of the scalar function $\Gamma_i(\varepsilon)$, we fix the energy argument in the numerators of the T matrix and interaction matrices at $\varepsilon = \varepsilon_0$, obtaining their forms

$$\hat{T}(\varepsilon) \approx \frac{\gamma^2\varepsilon_0}{\varepsilon^2 - \varepsilon_0^2}\hat{m}_+, \quad \hat{A}_{\mathbf{n}}(\varepsilon) \approx \hat{T}(\varepsilon)\frac{\varepsilon_0}{N}\sum_{\mathbf{k}}\frac{e^{i\mathbf{k}\cdot\mathbf{n}}}{D_{\mathbf{k}}(\varepsilon)}, \tag{28}$$

both proportional to the matrix $\hat{m}_+ = \hat{\sigma}_0 \otimes (\hat{\tau}_0 + \hat{\tau}_3)$ with an important multiplicative property: $\hat{m}_+^2 = 2\hat{m}_+$. The $\mathbf{k}$ summation (integration) in Eq. (28) is suitably done in polar coordinates over the circular segments of the Fermi surface. Here the azimuthal integration only refers to the phase of the numerator, resulting in a zeroth-order Bessel function: $\int_0^{2\pi} e^{ix\cos\theta}d\theta = 2\pi J_0(x)$. Since $x = n(k_F + \xi/\hbar v_F)$ is typically big, $x \gg 1$,

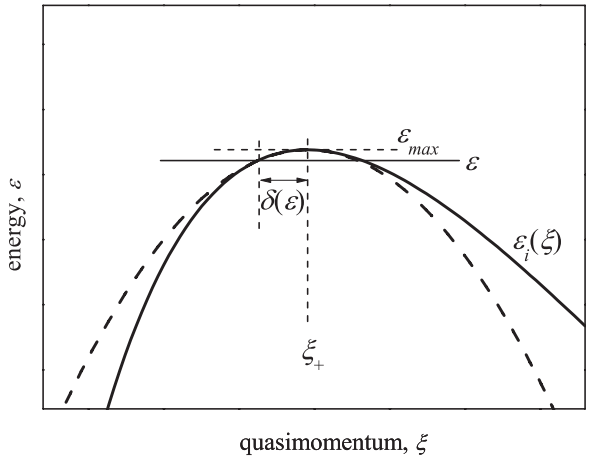

FIG. 5. Parabolic approximation (dashed line) for the dispersion law near the top of the impurity band (solid line), within the region indicated by the small rectangle in Fig. 3.

the asymptotical formula applies: $J_0(x) \approx \sqrt{2/(\pi x)}\cos(x - \pi/4)$. Then, for radial integration in ξ around the extremum point ξ_+, it is convenient to decompose this function in the fast and slow oscillating factors, $J_0(x) \approx \sqrt{2/(\pi k_+ n)}\cos(k_+ n - \pi/4)\cos[(\xi - \xi_+)\, n/\hbar v_F]$, with the fast wave number $k_+ = k_F + \xi_+/\hbar v_F \approx k_F$, and to write the denominator in the parabolic approximation: $D_\xi(\varepsilon) \approx (\xi - \xi_+)^2 - \delta^2(\varepsilon)$, with $\delta^2(\varepsilon) = 4\Delta\,(\Delta + \varepsilon_0)^2\,(\varepsilon_{\max} - \varepsilon)\,/(2c\gamma^2)$ (see Fig. 5). Thus, the interaction matrix $\hat{A}_{\mathbf{n}}(\varepsilon) = A_n(\varepsilon)\hat{m}_+$ depends only on the distance n between impurities, and for ε close to $\varepsilon_{\max}$, this dependence can be expressed as

$$A_r(\varepsilon) \approx \sqrt{\frac{r_\varepsilon}{r}}\sin k_\varepsilon r \cos k_F r, \tag{29}$$

where the length scales both for the monotonous decay,

$$r_\varepsilon = \frac{2\pi}{k_F}\left[\frac{\varepsilon_0 \rho_F\,(\Delta + \varepsilon_0)}{c\delta(\varepsilon)}\right]^2,$$

and for the sine factor, $k_\varepsilon^{-1} = \hbar v_F/\delta(\varepsilon)$, are much longer than k_F^{-1} for the fast cosine. The latter fast oscillation is specific for the interactions mediated by Fermi quasiparticles (like the known RKKY mechanism), unlike the monotonous or slowly oscillating interactions between impurities in semiconductors or in bosonic systems.[28] Now the calculation of $\Gamma_i(\varepsilon) = c^2 T(\varepsilon)\mathrm{Im}B(\varepsilon)$ mainly concerns the dominant scalar part of the GE pair term:

$$B(\varepsilon) \approx \frac{2\pi}{a^2}\int_a^{r_\varepsilon} \frac{r\,dr}{1 - 4A_r^2(\varepsilon)} \tag{30}$$

[since the **k**-dependent term in Eq. (18) turns out to be negligible beside this].

The upper integration limit in Eq. (30) corresponds to the condition that its integrand only has poles for $r < r_\varepsilon$. In conformity with the slow and fast modes in the function, Eq. (29) (see Fig. 6), the integration is naturally divided into two stages. In the first stage, integration over each mth period of fast cosine, around $r_m = 2\pi m/k_F$, is done by setting constant the slow factors, $r \approx r_m$ and $\sin k_\varepsilon r \approx \sin k_\varepsilon r_m$, and using the explicit formula

$$\mathrm{Im}\int_{-\pi}^{\pi} \frac{dx}{1 - 4A^2\cos^2 x} = \mathrm{Im}\frac{\pi}{\sqrt{1 - A^2}}. \tag{31}$$

In the second stage, the summation of these results in m is approximated by the integration in the slow variable:

$$\frac{\pi}{k_F}\mathrm{Im}\sum_m \frac{r_m^{3/2}}{\sqrt{r_m - r_\varepsilon \sin^2 k_\varepsilon r_m}} \approx \mathrm{Im}\int_a^{r_\varepsilon} \frac{r^{3/2}dr}{\sqrt{r - r_\varepsilon \sin^2 k_\varepsilon r}}. \tag{32}$$

The numerical calculation of the latter integral results in

$$\mathrm{Im}B = \frac{r_\varepsilon^2}{a^2} f\,(k_\varepsilon r_\varepsilon)\,, \tag{33}$$

where the function $f(z)$ is 0 for $z < z_0 \approx 1.3585$, and grows monotonously for $z > z_0$, rapidly approaching the asymptotic constant value, $f_{as} \approx 1.1478$, for $z \gg z_0$. Then the Ioffe-Regel-Mott criterion, Eq. (27), at ε so close to $\varepsilon_{\max}$ that $k_\varepsilon r_\varepsilon \gg z_0$, is expressed as

$$\varepsilon_{\max} - \varepsilon \gg \frac{c^2\gamma^2}{\varepsilon_{\max} - \varepsilon_0}\frac{r_\varepsilon^2}{a^2}, \tag{34}$$

and this would result in a (concentration-independent) estimate for the range of extended states within the impurity band,

$$\varepsilon_{\max} - \varepsilon \gg \Gamma_0 = \frac{(v\varepsilon_0)^{3/2}}{ak_F}\sqrt{\frac{2\pi\rho_F}{1 + v^2}}, \tag{35}$$

and its comparison with the full extension of this band, $\varepsilon_{\max} - \varepsilon_{\min} = c\gamma^2(1 + v^2)/(v^2\Delta)$, would suggest the possibility that such extended states really exist if the impurity concentration surpasses the characteristic (low) value:

$$c \gg c_0 = \frac{(\pi\rho_F\varepsilon_0)^{3/2}}{ak_F}\sqrt{\frac{2v}{1 + v^2}}. \tag{36}$$

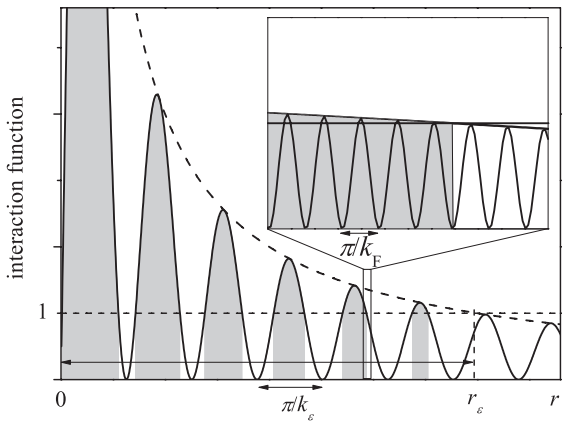

FIG. 6. Interaction function $A_r^2(\varepsilon)$ obtained with Eq. (29) with the choice of parameters $\varepsilon_{\max} - \varepsilon = 0.1$ and $\Delta/\varepsilon_F = 5 \times 10^{-2}$ displays slow sine oscillations (solid line) and the monotonous envelope function (dashed line). Shaded intervals are those contributing to $\mathrm{Im}B$, according to the condition $(r_\varepsilon/r)\sin^2 k_\varepsilon r > 1$. Inset: Expansion of the rectangle in the figure also shows fast oscillations by the cosine.

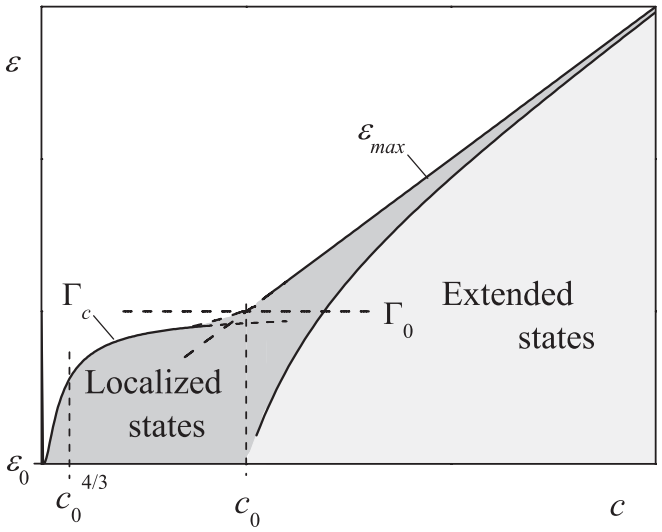

FIG. 7. Structure of the energy spectrum near the impurity level as a function of the impurity concentration.

For typical values of $\rho_F^{-1} \sim 2$ eV, $ak_F \sim 1$, and $\Delta \sim 10$ meV in the LaOFeAs system,[8,11,38] and supposing a plausible impurity perturbation $v \sim 1$, we estimate $c_0 \approx 8 \times 10^{-4}$, manifesting important impurity effects already at a very low content.

However, the right-hand side of Eq. (34) vanishes at $k_\varepsilon r_\varepsilon < z_0$, which occurs beyond the vicinity of the band top:

$$\varepsilon_{\max} - \varepsilon > \Gamma_0 \left(\frac{c_0}{c}\right)^3. \tag{37}$$

Under the condition of Eq. (36), this vicinity is even more narrow than Γ_0 obtained with Eq. (35), defining the true, even wider, range of extended states.

Otherwise, for $c \ll c_0$, the impurity band does not exist, thus we analyze the energy range near the impurity level with the nonrenormalized GE and write the approximate criterion for its convergence as $c|B^0| \ll 1$. This calculation is done in a similar way as before but replacing the interaction function, Eq. (29), with its nonrenormalized version:

$$A_r^0(\varepsilon) \approx \sqrt{R_\varepsilon / r}\, e^{-r/r_0} \cos k_F r, \tag{38}$$

with $k_F R_\varepsilon = 2\pi\, (\varepsilon_0/|\varepsilon - \varepsilon_0|)^2$ and $k_F r_0 = 2\varepsilon_F/\xi_0$. Then the above GE convergence criterion is assured beyond the following vicinity of impurity level:

$$|\varepsilon - \varepsilon_0| \gg \Gamma_c = \Gamma_0 \exp\left(-c_0^{4/3}/c\right), \tag{39}$$

defining the range of its broadening due to interimpurity interactions. The DOS function for localized states can be only estimated by the order of magnitude within this range, but outside is given by

$$\begin{aligned} \rho_{\rm loc}(\varepsilon) &\approx \frac{c^2}{c_0^{4/3}|\varepsilon - \varepsilon_0|}, \quad \text{for} \quad \Gamma_c \ll |\varepsilon - \varepsilon_0| \ll \Gamma_0, \\ \rho_{\rm loc}(\varepsilon) &\approx \frac{c^2 \varepsilon_0^4}{|\varepsilon - \varepsilon_0|^5}, \quad \text{for} \quad \Gamma_0 \ll |\varepsilon - \varepsilon_0|. \end{aligned} \tag{40}$$

Notably, the total number of states near the impurity level is $\int \rho_{\rm loc}(\varepsilon) d\varepsilon \sim c$, like that of extended states in the impurity band obtained with Eq. (26). A summary of the evolution of this area of the quasiparticle spectrum as a function of the impurity concentration is shown in Fig. 7.

VI. IMPURITY EFFECTS ON SC CHARACTERISTICS

The above results on the quasiparticle spectrum in a disordered SC system can be used immediately for calculation of impurity effects on its observable characteristics. Thus the fundamental SC order parameter Δ is estimated from the modified gap equation,

$$\lambda^{-1} = \int_0^{\varepsilon_D} \rho(\varepsilon) d\varepsilon, \tag{41}$$

where $\lambda = \rho_F V_{SC}$ is the (small) dimensionless SC pairing constant and the Debye energy ε_D restricts the energy range of its action. In the absence of impurities, $c = 0$, using the BCS DOS in this equation leads straightforwardly to the known result for its nonperturbed value Δ_0, $\lambda^{-1} = \operatorname{arcsinh}(\varepsilon_D/\Delta_0)$, and thus to $\Delta_0 \approx \varepsilon_D e^{-1/\lambda}$.

For finite c, the total DOS is the combined contributions from the shifted main band ρ_b, Eq. (25), and from the impurity band (or level) ρ_i (or $\rho_{\rm loc}$), Eq. (26) [or (40)]. The latter contribution is $\sim$c, according to the previous discussion, defining a small correction besides $\lambda^{-1} \gg 1$. But a much stronger c-dependent correction comes from the modified main band:

$$\int_{\Delta_c}^{\varepsilon_D} \rho_b(\varepsilon) d\varepsilon \approx \operatorname{arcsinh}\frac{\varepsilon_D}{\Delta_c} - c\gamma^2 \int_{\Delta_c}^{\varepsilon_D} \frac{d\varepsilon}{(\varepsilon - \varepsilon_0)^2 \sqrt{\Delta_c^2 - \varepsilon^2}}.$$

For $\varepsilon_D \gg \Delta_c$, the last integral is well approximated by

$$c\gamma^2 \int_{\Delta_c}^{\infty} \frac{d\varepsilon}{(\varepsilon - \varepsilon_0)^2 \sqrt{\Delta_c^2 - \varepsilon^2}} = \frac{c\gamma^2}{\Delta_c^2} F\left(\frac{\Delta_c}{\varepsilon_0}\right),$$

with the function

$$F(z) = z \frac{\sqrt{z^2 - 1} + z \arccos(-1/z)}{(z^2 - 1)^{3/2}}.$$

This F diverges at $z \to 1$, but actually its argument,

$$\Delta_c/\varepsilon_0 = \sqrt{1 + v^2}(1 + c/c_1), \quad \text{with} \quad c_1 = \pi \rho_F \Delta / v,$$

is always above unity. Neglecting the small ρ_i contribution in Eq. (41) and taking account of the BCS relation $\lambda^{-1} = \operatorname{arcsinh}(\varepsilon_D/\Delta_0)$, we express the gap equation as

$$\operatorname{arcsinh}\frac{\Delta_c - \Delta_0}{\Delta_0} \approx \frac{cv^2}{c_1(1 + v^2)} F(\Delta_c/\varepsilon_0). \tag{42}$$

Its approximate solution for $c \ll c_1$, together with the relation $\Delta_c/\Delta = 1 + c/[c_1(1 + v^2)]$, leads to the desired expression for the perturbed SC order parameter Δ:

$$\frac{\Delta}{\Delta_0} \approx 1 - \frac{c}{c_1} \frac{1 + v^2 F[\sqrt{1 + v^2}(1 + c/c_1)]}{1 + v^2}, \tag{43}$$

which rapidly decays with impurity concentration and would vanish at

$$c = c_1 \frac{1 + v^2}{1 + v^2 F[\sqrt{1 + v^2}(1 + c/c_1)]}.$$

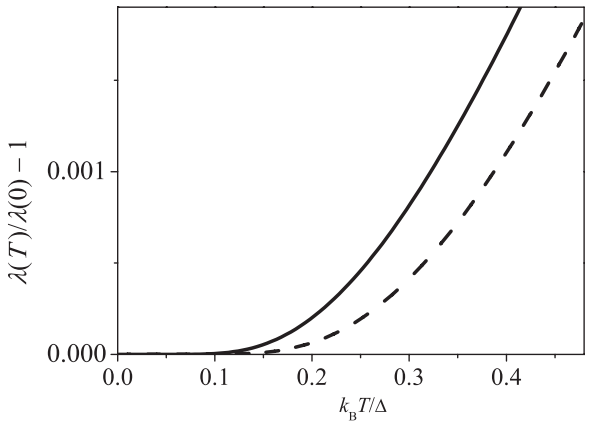

FIG. 8. Low-temperature decay of the London penetration depth difference for an SC with impurities (solid line) is slower than that in the absence of impurities (dashed line).

The latter equality in fact defines a certain equation for c and its solution, e.g., for the above choice of $v = 1$, is $c \approx 0.5c_1 \approx 6 \times 10^{-3}$. However, such concentrations would already correspond to an impurity band as wide as the gap itself; this goes beyond the validity of the above derivation and requires special treatment (to be done elsewhere).

To study another important dependence, that of the SC transition temperature T_c on the concentration c, one must, strictly speaking, extend the above GF techniques to finite temperatures, but a very simple estimate can be done, supposing that the BCS relation $\Delta/T_c \approx 1.76$ still holds in the presence of impurities. Then the right-hand side of Eq. (43) would also describe the decay of T_c/T_{c0}.

It is of interest to compare the present results with the known Abrikosov-Gor'kov solution for BCS SC with paramagnetic impurities in the Born approximation.[39,40] In that approximation, the only perturbation parameter is the (constant) quasiparticle lifetime τ. In our framework, the τ^{-1} can be related to $\mathrm{Im}\Sigma(\varepsilon)$ at a proper choice of energy, $\varepsilon \sim |\Delta - \varepsilon| \sim \Delta$. Then, in the self-consistent T-matrix approximation,[31] we estimate $\tau^{-1} \sim c\Delta/c_1$, which leads to the relation $\tau T_c \sim c_1/c$, reaching, at $c \gtrsim c_1$, qualitative agreement with the Abrikosov-Gor'kov universal criterion for complete SC suppression $\tau T_c < 0.567$ (though in our case this criterion is not universal and still depends on the perturbation parameter v).

Also, a notable impurity effect on the London penetration depth $\lambda_L \sim n_s^{1/2}$ is expected, as follows from the temperature dependence of the superfluid density:

$$n_s(T) = \int_0^\infty \frac{\rho(\varepsilon)d\varepsilon}{e^{\varepsilon/k_BT}+1} \approx \frac{c}{e^{\varepsilon_0/k_BT}+1} + \left(1 - \frac{c\gamma^2}{\Delta^2 - \varepsilon_0^2}\right) n_s^0(T). \quad (44)$$

Compared to its unperturbed value in the pure SC system,

$$n_s^0(T) = \rho_F \int_\Delta^\infty \frac{\varepsilon d\varepsilon}{(e^{\varepsilon/k_BT}+1)\sqrt{\varepsilon^2 - \Delta^2}} \approx \pi\rho_F \sqrt{\frac{k_BT\Delta}{2}} e^{-\Delta/k_BT},$$

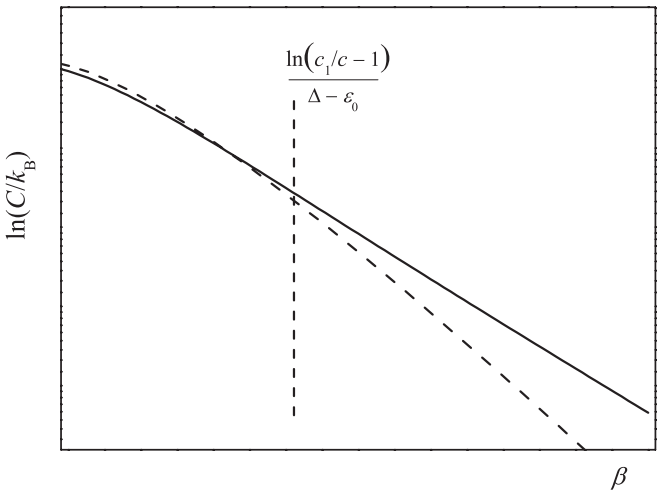

FIG. 9. The temperature behavior of specific heat for an SC with impurities presents a crossover from the $\beta\Delta$ exponent (dashed line) to $\beta\varepsilon_0$ at a low enough temperature (high enough $\beta = 1/k_BT$).

a considerable slowing-down of the low-temperature decay of the characteristic difference $\lambda(T)/\lambda(0) - 1$ is displayed (Fig. 8), in reasonable agreement with recent experimental observations for SC ferropnictides under doping.[41]

Finally, a similar analysis can be applied to the impurity effect on the electronic specific heat in the SC state, whose dependence on the inverse temperature $\beta = 1/k_BT$ is represented as

$$C(\beta) = \frac{\partial}{\partial T}\int_0^\infty \frac{\rho(\varepsilon)d\varepsilon}{e^{\beta\varepsilon}+1}, \quad (45)$$

and naturally divided into two characteristic contributions, $C = C_i + C_b$, from the ρ_i and ρ_b states:

$$C_i(\beta) \approx k_Bc\left[\frac{\beta\varepsilon_0}{2\cosh(\beta\varepsilon_0/2)}\right]^2$$

and

$$C_b(\beta) \approx k_B(c_1 - c)v(\beta\Delta_c)^{3/2}\exp(-\beta\Delta_c).$$

The resulting function $C(\beta)$ deviates from the known low-temperature behavior $C_0(\beta) \sim \exp(-\beta\Delta)$ for a nonperturbed SC system at $\beta > \ln(c_1/c - 1)/(\Delta - \varepsilon_0)$, where the characteristic exponent is changed to the slower $\sim\exp(-\beta\varepsilon_0)$ as shown in Fig. 9.

The same approach can be used for calculation of other observable characteristics for the SC state under impurity effects, e.g., heat conductivity, differential conductivity for scanning tunneling spectroscopy, and absorption coefficient for far-infrared radiation, although these issues are beyond the scope of this work.

VII. CONCLUSIONS

In summary, the GF analysis of quasiparticle spectra in an SC ferropnictide with impurities of the simplest (local and nonmagnetic) perturbation type permits us to describe the formation of impurity localized levels within the SC gap and, with increasing impurity concentration, their evolution to specific bands of extended quasiparticle states, approximately

described by the quasimomentum but mainly supported by the impurity centers. Explicit dispersion laws and DOS are obtained for the modified main bands and impurity bands. Further specification of the nature of all the states in different energy ranges within the SC gap is obtained through analysis of different types of GEs for a self-energy matrix, revealing a complex oscillatory structure of indirect interactions between impurity centers and, after their proper summation, resulting in criteria for crossovers between localized and extended states. The developed spectral characteristics are applied to the prediction of several observable impurity effects. The proposed treatment can be further adapted for analysis of more involved types of impurity perturbations in SC ferropnictides, including magnetic and nonlocal perturbations.

ACKNOWLEDGMENTS

Y.G.P. and M.C.S. acknowledge the support of this work through Portuguese FCT project PTDC/FIS/101126/2008. V.M.L. is grateful to the Special Program of Fundumental Research of the NAS of Ukraine.

*ypogorel@fc.up.pt

[1] Y. Kamihara, H. Hiramatsu, M. Hirano, R. Kawamura, H. Yanagi, T. Kamiya, and H. Hosono, J. Am. Chem. Soc. **128**, 10012 (2006).
[2] Y. Kamihara, T. Watanabe, M. Hirano, and H. Hosono, J. Am. Chem. Soc. **130**, 3296 (2008).
[3] M. V. Sadovskii, Phys. Usp. **51**, 1201 (2008).
[4] Yu. A. Izyumov and E. Z. Kurmaev, Phys. Usp. **51**, 1261 (2008).
[5] D. M. Ginsberg, ed., *Physical Properties of High Temperature Superconductors I* (World Scientific, Singapore, 1989).
[6] H. Takahachi, K. Igawa, K. Arii, Y. Kamihara, M. Hirano, and H. Hosono, Nature **453**, 376 (2008).
[7] M. R. Norman, Physics **1**, 21 (2008).
[8] H. Ding, P. Richard, K. Nakayama, K. Sugawara, T. Arakane, Y. Sekiba, A. Takayama, S. Souma, T. Sato, T. Takahashi, Z. Wang, X. Dai, Z. Fang, G. F. Chen, J. L. Luo, and N. L. Wang, Europhys. Lett. **83**, 47001 (2008).
[9] T. Kondo, A. F. Santander-Syro, O. Copie, C. Liu, M. E. Tillman, E. D. Mun, J. Schmalian, S. L. Budko, M. A. Tanatar, P. C. Canfield, and A. Kaminski, Phys. Rev. Lett. **101**, 147003 (2008).
[10] D. J. Singh and M.-H. Du, Phys. Rev. Lett. **100**, 237003 (2008).
[11] K. Haule, J. H. Shim, and G. Kotliar, Phys. Rev. Lett. **100**, 226402 (2008).
[12] G. Xu, W. Ming, Y. Yao, X. Dai, S.-C. Zhang, and Z. Fang, Europhys Lett. **82**, 67002 (2008).
[13] I. I. Mazin, D. J. Singh, M. D. Johannes, and M. H. Du, Phys. Rev. Lett. **101**, 057003 (2008).
[14] C. Cao, P. J. Hirschfeld, and H. P. Cheng, Phys. Rev. B **77**, 220506 (2008).
[15] S. Raghu, X. L. Qi, C. X. Liu, D. J. Scalapino, and S. C. Zhang, Phys. Rev. B **77**, 220503 (2008).
[16] K. Kuroki, S. Onari, R. Arita, H. Usui, Y. Tanaka, H. Kontani, and H. Aoki, Phys. Rev. Lett. **101**, 087004 (2008).
[17] A. V. Chubukov, D. V. Efremov, and I. Eremin, Phys. Rev. B **78**, 134512 (2008).
[18] L. Boeri, O. V. Dolgov, and A. A. Golubov, Phys. Rev. Lett. **101**, 026403 (2008).
[19] Q. Si and E. Abrahams, Phys. Rev. Lett. **101**, 076401 (2008).
[20] M. Daghofer, A. Moreo, J. A. Riera, E. Arrigoni, D. J. Scalapino, and E. Dagotto, Phys. Rev. Lett. **101**, 237004 (2008).
[21] W. F. Tsai, Y. Y. Zhang, C. Fang, and J. Hu, Phys. Rev. B **80**, 064513 (2009).
[22] S. Graser, P. J. Hirschfeld, T. Maier, and D. J. Scalapino, New J. Phys. **81**, 45 (2009).
[23] T. A. Maier, S. Graser, D. J. Scalapino, and P. J. Hirschfeld, Phys. Rev. B **79**, 224510 (2009).
[24] D. Zhang, Phys. Rev. Lett. **103**, 186402 (2009).
[25] Y. Y. Zhang, C. Fang, X. Zhou, K. Seo, W. F. Tsai, B. A. Bernevig, and J. Hu, Phys. Rev. B **80**, 094528 (2009).
[26] P. W. Anderson, J. Phys. Chem. Solids **11**, 26 (1959).
[27] M. A. Ivanov and Y. G. Pogorelov, JETP **61**, 1033 (1985).
[28] M. A. Ivanov, V. M. Loktev, and Y. G. Pogorelov, Phys. Rep. **153**, 209 (1987).
[29] A. V. Balatsky, M. I. Salkola, and A. Rosengren, Phys. Rev. B **51**, 15547 (1995).
[30] Y. G. Pogorelov, Solid State Commun. **95**, 245 (1995).
[31] Y. G. Pogorelov, M. C. Santos, and V. M. Loktev, *Strongly Correlated Systems, Coherence and Entanglement* (World Scientific, Singapore, 2007), p. 443.
[32] E. N. Economou, *Green's Functions in Quantum Physics* (Springer, Berlin, 2006).
[33] S. Onari and H. Kontani, Phys. Rev. Lett. **103**, 177001 (2009).
[34] D. V. Efremov, M. M. Korshunov, O. V. Dolgov, A. A. Golubov, and P. J. Hirschfeld, e-print arXiv:1104.3840 (2011).
[35] M. Tinkham, *Introduction to Superconductivity* (McGraw–Hill, New York 1995).
[36] A. F. Ioffe and R. A. Regel, Prog. Semicond. **4**, 237 (1960).
[37] N. F. Mott, Adv. Phys. **16**, 49 (1967).
[38] I. Mazin and J. Schmalian, Physica C **469**, 614 (2009).
[39] M. J. DeWeert, Phys. Rev. B **38**, 732 (1988).
[40] R. V. A. Srivastava and W. Teizer, Solid State Commun. **145**, 512 (2008).
[41] R. T. Gordon, H. Kim, M. A. Tanatar, R. Prozorov, and V. G. Kogan, Phys. Rev. B **81**, 180501 (2010).